Electronic Supplementary Material (ESI) for Chemical Communications.

Supporting Information for

Coordination promiscuity guarantees metal substrate selection in transmembrane primary-active Zn^{2+} pumps

Marc Joseph Gallenito[1#], Gordon William Irvine[1#], Limei Zhang[2], Gabriele Meloni[1]

[1]Department of Chemistry and Biochemistry, The University of Texas at Dallas, Richardson, TX 75080, USA
[2]Department of Biochemistry and §Redox Biology Center and the Nebraska Center for Integrated Biomolecular Communication, University of Nebraska—Lincoln, Lincoln, NE 68588, USA

To whom correspondence should be addressed: gabriele.meloni@utdallas.edu

[#] These authors contribute equally to this work

Material and Methods

Generation of the ΔZntA$_{121-740}$ construct and protein expression - A construct coding for the sequence corresponding to the N-terminal deletion mutant ΔZntA$_{121-740}$ with an N-terminal hexa-histidine tag was generated by polymerase chain reaction from the cDNA coding for full-length ZntA from *Pseudomonas aeruginosa* The product was cloned into a modified pET19b vector containing a thrombin cleavage site for tag removal and transformed in to *E. coli* BL21(DE3) GOLD strains for recombinant protein expression. The transformed cells were grown at 37 °C in Terrific Broth (TB)-glycerol media containing 50 μg/ml ampicillin until an OD_{600nm} = 2 was reached, and then cooled at 23 °C for 30 min. Protein expression was induced by the addition of isopropyl thiogalactopyranoside (IPTG) to a final concentration of 0.1 mM. Cells were harvested 18 h post-induction by centrifugation at 9000 g, and 4 °C, 20 min, and then stored at -80 °C. C391A, C393A, C391A/C393A, D721A and D721N mutants were generated by site-directed mutagenesis (Genescript Inc.) and expressed and purified using the same protocols utilized for *Pa*ΔZntA$_{121-740}$.

Protein purification- Cells were suspended in buffer A (20 mM Tris HCl pH 8, 150 mM NaCl, 5 mM $MgCl_2$) supplemented with 30 μg/ml of DNaseI from bovine pancreas (Sigma-Aldrich) and an EDTA-free protease inhibitor cocktail (Roche) to a final concentration of 0.1 g cells mL^{-1}. Cells were disrupted by 3-pass cycles through a microfluidizer operating at a pressure of 18000–20000 psi. Membranes were collected by ultracentrifugation (1 h, 4 °C, 185000 g), and washed to a concentration of 0.5 g of original cells per mL of buffer in 20 mM Tris/HCl pH 8, 500mM NaCl, EDTA-free protease inhibitor cocktail (Roche). Membranes were further collected by ultracentrifugation (1 h, 4 °C, 185000 g) and suspended to a final concentration of 1 g of original cells per mL in 20 mM Tris/HCl pH 8, 500 mM NaCl, 10 % (w/v) glycerol.

His_6-ΔZntA was purified by affinity chromatography using Ni-NTA affinity resin with a 5 mL HisTrap Column (GE Health care) or by custom-packed gravity columns upon batch binding to NiNTA Superflow resin. Typically, membranes from 10 g of cells were diluted to 50 mL in ice-cold 20 mM Tris HCl pH 8, 500 mM NaCl, 25 mM imidazole, 5 mM mercaptoethanol, and EDTA-free protease inhibitor cocktail (Roche). Proteins were extracted by addition of 1 % (w/v) 7-cyclohexyl-1-heptyl-β-D-maltoside (Cymal-7) detergent and stirred for 1 h at 4 °C. Insoluble material and residual membranes were removed by ultracentrifugation (30 min, 4 °C, 185000 g)

and the supernatant was either loaded onto a 5mL HisTrap affinity column at a flow rate of 0.5 ml min^{-1} bound or by batch binding to 10 mL of NiNTA Superflow resin under stirring. The resin was washed with 30 column volumes of 20 mM Tris/HCl pH 8, 500 mM NaCl, 25 mM imidazole, 0.05 % Cymal-7, and 1 mM dithiothreitol (DTT). The protein was eluted with 20 mM Tris/HCl pH 8, 500 mM NaCl, 250 mM imidazole, 0.05 % (w/v) Cymal-7, 1 mM DTT and the imidazole was immediately removed using a Hi prep 26 10 desalting column connected to an Akta FPLC system by elution in 20 mM Tris/HCl pH 8, 500 mM NaCl, 0.05 % (w/v) Cymal-7, 1 mM DTT for His_6-tag removal by thrombin cleavage, or in 20 mM MES pH 6, 500 mM NaCl, 0.05 % (w/v) Cymal-7, 1 mM DTT, and 1 mM EDTA for further reconstitution in proteoliposomes.

Thrombin digestion was performed at 4 °C for 22 h. Upon diluting the purified protein to final concentration of 0.2 mg/mL, restriction grade purified human Thrombin (Novagen) was added at a concentration of 0.25–0.5 U /mL.

The purified protein was concentrated with a 100 kDa molecular weight cutoff (MWCO) membrane using Amicon spinning devices to a final concentration of ~5–10 mg/mL and subsequently loaded onto a size exclusion chromatography Superdex 200 10/30 column to remove protein aggregates, thrombin and degradation products, and eluted with argon-saturated 20 mM Tris/HCl pH 8, 500 mM NaCl, 0.05% (w/v) Cymal-7 or 20 mM MES pH 6, 500 mM NaCl, 0.05 (w/v)% Cymal-7. Protein concentration determination was performed based on tyrosine and tryptophan absorption at 280 nm using a calculated extinction coefficient ε_{280} = 69940 M^{-1} cm^{-1}. Protein purity was assessed by SDS-PAGE.

Determination of metal binding stoichiometry by inductively coupled plasma mass Spectrometry (ICP-MS)

$\Delta ZntA_{121\text{-}740}$ was titrated with 3–4 molar equivalents of $ZnCl_2$, and subsequently desalted using a 5 mL Hi Trap desalting columns packed with Sephadex G-25 resin to remove free or loosely bound metal. The eluted protein was quantified by its UV absorption at 280 nm and metal concentration was determined by inductively coupled plasma mass spectrometry (ICP-MS).

For ICP-MS, protein samples were mixed with concentrated HNO_3 (69% w/v) to an HNO_3 concentration of 10% (w/v) and digested at 80 °C for 2 h. The samples were subsequently diluted to a final concentration of 1% HNO_3. ICP-MS was performed using a Hewlett-Packard 4500 ICP mass spectrometer (Agilent Technologies, Caltech Environmental Analysis Center) connected to

a CETAC ASX-500 auto-sampler for sample injection. The protein-free buffer (20 mM MES pH 6, 500 mM NaCl, 0.05% (w/v) Cymal-7) was used for background blank subtraction. High-purity TraceSelect nitric acid, metal standards and TraceSelect H_2O were from purchased from Sigma-Aldrich.

Reconstitution of *Pa*ΔZntA$_{121-740}$ in proteoliposomes - *E. coli* polar lipids (25 mg/mL) and egg-yolk phosphatidyl choline (25 mg/mL) in chloroform were mixed in a 3:1 ratio (w/w) and dried under a nitrogen stream and continuous rotation to form a homogeneous thin film in a glass balloon. The lipid mixture was desiccated overnight under vacuum (protected from light) and subsequently suspended in a 1 mM DTT solution. A concentrated stock was used to bring the suspension to a final concentration of 20 mM MES pH 6, 250 mM NaCl and 1 mM DTT. The prepared lipids were subjected to three rounds of freeze-thawing in liquid N_2. Proteoliposomes were prepared by extrusion (11 times) through 0.2 μm polycarbonate filters to form large unilamellar vesicles (LUVs) using a mini extruder (Avanti Polar Lipids) equipped with two 1 mL gas-tight syringes. Proteoliposomes were destabilized by addition of Cymal-7 to a final concentration of 0.02% (w/v) and tilting for 1 h at 18 °C, and subsequently were placed on ice for 10 min. Purified *Pa*ΔZntA$_{121-740}$ (1–2 mg/mL), purified essentially as described for crystallization, was added to a final protein-to-lipid ratio of 1:75 (w/w) for ATPase activity determinations, or 1:20 (w/w) for XAS sample preparations and the mixture was incubated for 1 h at 4 °C under tilting. Control liposomes were prepared using the same procedure without addition of protein. Detergent was removed through consecutive incubations with activated Bio-Beads SM-2 (BioRad), by exchanging the beads after 1, 16, 18 and 20 h. The Bio-beads were subsequently removed, proteoliposomes collected by ultracentrifugation at 163,000 g for 45–60 min at 4 °C, and suspended in 20 mM MES pH 6, 250 mM NaCl, 1 mM DTT (Buffer PL) to a final protein concentration of 0.5–2 mg/mL.

Determination of ATPase activity and metal selectivity in wt*Pa*ZntA and *Pa*ΔZntA$_{121-740}$ in detergent micelles - ATP hydrolysis associated with ATPase activity was measured using the malachite green assay[1]. Briefly, stock solutions of wt*Pa*ZntA and ΔZntA$_{121-740}$ were diluted to 0.5–0.7 mg/mL using buffer with final composition of 20 mM MES-NaOH pH 6.0, 500 mM NaCl, 5 mM $MgCl_2$, 0.05% (w/v) Cymal-7 and 1 mM DTT. To test Zn^{2+} dependent ATPase activity, stock

solutions of Zn were added to final concentrations of 5–80 μM to 40 μL protein samples. Non-linear curve fitting using a Michaelis-Menten-type equation was performed to calculate V_{max} and K_M using Originlab software. For metal selectivity ATPases assays, stock solutions of metal salts ($Pb(CH_3COO)_2$, $ZnCl_2$, $HgCl_2$, $CdCl_2$, $MnCl_2$, $NiCl_2$, $CoCl_2$ or $CuCl_2$) or EDTA were added to a final concentration of 40 μM. ATP was added to initiate the reaction (Na_2ATP, 2.0 mM final concentration) and samples were incubated in a 96-well plate at 30 °C, shaking at 350 rpm for 45 min. Then, 134 μL of malachite green reagent (0.045% (w/v) malachite green-C_2O_4, 4.2% (w/v) $(NH_4)_6Mo_7O_{24}$-$7H_2O$, 0.05% (w/v) Triton X-100 and 0.1% (w/v) Cymal-7 in 1.0 M HCl) was added to the protein assay solution. The solutions were then incubated with 16.5 uL of 1.5 M sodium citrate for 30 min. Absorbance at 650 nm was measured using a Tecan Spark 20M plate reader. The inorganic phosphate produced was calculated using a Pi standard curve and corrected against the hydrolysis of ATP in the absence of the enzyme.

Relative ATPase activity on C391A, C393A, C391A/C393A, D721A and D721N mutants was determined using the Malachite green assay kit (see next paragraph) using a similar protocol.

Determination of the specific ATPase activity of wt*Pa*ZntA and *Pa*ΔZntA$_{121\text{-}740}$ in proteoliposomes

ATP hydrolysis was measured using a Malachite green assay kit (Sigma-Aldrich, USA) according to the manufacturer's instructions. The reaction mixture containing 20 mM MES pH 6, 250 mM NaCl, 1 mM DTT containing 1 mM ATP, 10 mM $MgCl_2$, proteoliposome suspension (diluted to 0.2–0.25 mg/ml), and varying $ZnCl_2$ concentrations (total volume 40 μL) was placed in a reaction shaker (Eppendorf ThermoMixer) at 30 °C for 45 min. Subsequently, the reacted mixtures were centrifuged (17000 g, 4 °C, 15 min) and the supernatant was collected to remove light scattering by the proteoliposomes. The Malachite green assay kit solution was added to the supernatant, incubated at room temperature for 30 min, and the absorbance measured at 620 nm (Biotek Synergy H4 plate reader).

The ATPase activity was calculated using standard curves generated from inorganic phosphate standards on the same plate and the amount of free phosphate was normalized to a control solution without Zn to account for background ATP hydrolysis. Each point was obtained by averaging at least three experiments and the error bars represent the standard deviation.

Determination of metal selectivity via ATPase activity in *Pa*ΔZntA$_{121-740}$ proteoliposomes - ATPase activity was measured for 40 min at 37 °C upon incubation of ΔZntA$_{121-740}$ proteoliposomes (ΔZntA$_{121-740}$ concentration ~ 0.4 mg/mL) in 20 mM MES pH 6, 250 mM NaCl, 1 mM DTT with 10 mM $MgCl_2$ and 1 mM ATP in the presence of 40 µM $Pb(CH_3COO)_2$, $ZnCl_2$, $HgCl_2$, $CdCl_2$, $MnCl_2$, $NiCl_2$, $CoCl_2$ or $CuCl_2$. Released inorganic phosphate (Pi) was determined using the Malachite Green assay[1] with KH_2PO_4 standards for calibration by determining the absorption at 650 nm in a 96-well plate reader (Infinite series 200, Tecan). ATP hydrolysis in the presence of 500 µM AlF_4^-, 500 µM VO_4^{3-}, or 100 µM ouabain was also tested using the Malachite Green assay. AMPPCP hydrolysis was tested upon incubation with 1 mM AMPPCP under the same conditions.

Cd^{2+} titration monitored by UV-Vis absorption spectroscopy - *Pa*ΔZntA$_{121-740}$ (1.5 µM) in 20 mM Tris pH 8, 500 mM NaCl, 0.05 % (w/v) Cymal-7 was titrated with a $CdCl_2$ stock solution in H_2O followed by electronic absorption spectroscopy. UV–Vis absorption spectra were recorded on a Cary 3 spectrophotometer (Varian Inc.) using 10 mm quartz cuvettes. All solutions used in the experiments were saturated with argon prior to use.

XAS sample preparation - ΔZntA$_{121-740}$–Zn^{2+}, ΔZntA$_{121-740}$–Cd^{2+}, ΔZntA$_{121-740}$–Hg^{2+} and ΔZntA$_{121-740}$–Pb^{2+} in detergent micelles solutions were generated by addition of 1 molar equiv. of $ZnCl_2$, $CdCl_2$, $HgCl_2$ or $Pb(CH_3COO)_2$ to the purified *Pa*ΔZntA$_{121-740}$ in 20 mM Tris-HCl pH 8, 500 mM NaCl, 0.05 % (w/v) Cymal-7 and 20 % (w/v) glycerol. The samples were concentrated to 0.4–0.6 mM, and loaded into custom-made polycarbonate XAS sample cells (Vantec, Canada), sealed with metal-free tape, flash frozen in liquid nitrogen and stored in liquid nitrogen until data collection.

Proteoliposome preparations for XAS measurements were generated using a different protocol. Reconstituted *Pa*ΔZntA$_{121-740}$ proteoliposomes were collected by ultracentrifugation (163,000 g for 45-60 min at 4 °C) and suspended in 20 mM MES, 500mM NaCl, 10mM $MgCl_2$ to a final protein concentration of approximately 20 µM in the presence of $ZnCl_2$, $CdCl_2$, $Pb(CH_3COO)_2$ or $Hg\ Cl_2$ (25 µM). The proteoliposomes were collected by ultracentrifugation (163,000 g, 60 min, 4 °C) and were subsequently washed in 1–3 mL of buffer without metal and collected by an additional ultracentrifugation step. Proteoliposome pellets were loaded using a metal micro-

spatula into custom-made polycarbonate XAS sample cells, flash frozen in liquid nitrogen and stored in liquid nitrogen until data collection.

XAS data collection and analysis - X-ray absorption spectroscopy measurements were performed at the Stanford Synchrotron Radiation Lightsource with the SPEAR 3 storage ring of 450-500 mA at 3.0 GeV. Zinc and cadmium K-edge data, as well as lead and mercury L_3-edge data were collected at beamlines 7-3 and 9-3 with a wiggler field of 2 Tesla and employing an Si(220) double-crystal monochromator and a vertically-collimating pre-monochromator harmonic rejection mirror. Alternatively, for cadmium K-edge data collection at beamline 7-3, harmonic removal was achieved by detuning the monochromator crystal by 50%. The incident and transmitted X-ray intensities were monitored using nitrogen-filled ionization chambers and X-ray absorption was measured by monitoring the fluorescence yield using an array of 30 germanium detectors (100 Ge detectors for beamline 9-3).

Copper, silver, arsenic or selenium filters were placed between the cryostat and the germanium detector to reduce scattered X-rays not associated with Zn, Cd, Hg or Pb fluorescence, respectively. During data collection, the samples were maintained at a temperature of ~10 K using an Oxford instruments liquid helium flow cryostat.

The Zn XAS spectra were measured using 10 eV steps in the pre-edge region (9430–9640 eV), 0.35 eV steps in the edge region (9640–9690 eV) and 0.05 $Å^{-1}$ increments in the EXAFS region (to $k = 14.2$ $Å^{-1}$). A total of 8 ~ 40-min scans were accumulated, and the energy was calibrated by reference to the absorption of a standard Zn metal foil measured simultaneously with each scan, assuming a lowest energy inflection point of the zinc foil at 9660.7 eV.

The Cd XAS spectra were measured using 10 eV steps in the pre-edge region (26500–26680 eV), 0.5 eV steps in the edge region (26680–26750 eV) and 0.05 $Å^{-1}$ increments in the EXAFS region (to $k = 14.2$ $Å^{-1}$). A total of 8–12 ~ 40-min scans were accumulated, and the energy was calibrated by reference to the absorption of a standard Cd metal foil measured simultaneously with each scan, assuming a lowest energy inflection point of the cadmium foil at 26714.0 eV.

The Hg XAS spectra were measured using 10 eV and 1eV steps in the pre-edge region (12150–12240 and 12240–12265 eV, respectively), 0.35 eV steps in the edge region (12265–12350eV) and 0.05 $Å^{-1}$ increments in the EXAFS region (to $k = 14.2$ $Å^{-1}$). A total of 10–12 ~40-min scans were accumulated, and the energy was calibrated by reference to the absorption of a standard

$HgCl_2$ sample measured simultaneously with each scan, assuming a lowest energy inflection point of the reference at 12285.0 eV.

The Pb XAS spectra were measured using 10 eV steps in the pre-edge region (12810–13020eV), 0.35 eV steps in the edge region (13020–13070eV) and 0.05 $Å^{-1}$ increments in the EXAFS region (to k = 13.2 $Å^{-1}$). A total of 10-18 ~40-min scans were accumulated, and the energy was calibrated by reference to the absorption of a standard lead metal foil measured simultaneously with each scan, assuming a lowest energy inflection point of the lead foil at 13038.0 eV.

The extended X-ray absorption fine structure (EXAFS) oscillations (k) were quantitatively analyzed by curve fitting using the EXAFSPAK suite[2]. *Ab initio* theoretical phase and amplitude functions were calculated using the program FEFF version 8.2[3]. Data obtained from each Ge-detector element were checked and data from elements showing abnormal responses were excluded from data averaging. No smoothing, filtering, or related operations were performed on the data.

3D structure homology modeling - The homology model for wt*Pa*ZntA (residues 51–740) was calculated using the Robetta Protein Structure Prediction Server (http://robetta.bakerlab.org/) basing the homology on the *Archeoglobus Fulgidus* CopA model obtained by cryo-EM (PDB 3J09).

References

1. Lanzetta, P. A., Alvarez, L. J., Reinach, P. S., Candia, O. A. (1979), An improved assay for nanomole amounts of inorganic phosphate *Anal. Biochem. 100*, 95–97
2. George, G.N., http://ssrl.slac.stanford.edu/exafspak.html.
3. Ankudinov, A.L., Ravel, B., Rehr J.J., Conradson S.D. (1998) Real-space multiple-scattering calculation and interpretation of x-ray-absorption near-edge structure *Phys. Rev. B*, *58*, 7565–7576

Acknowledgements

The work was supported by the Robert A. Welch Foundation (AT-1935-20170325 to G.M), by the National Institute Of General Medical Sciences of the National Institutes of Health (R35GM128704 to G.M.) and by a Marie Curie Fellowship (European Commission, No. 252961 to G.M.). This work was also supported by P30 GM103335 to L. Z. through the Nebraska Redox Biology Center. G.W.I. is supported by an NSERC postdoctoral fellowship (PDF; Natural Sciences and Engineering Research Council of Canada). We thank the staff at Beamline 7-3/9-3,

Stanford Synchrotron Radiation Lightsource (SSRL) for support in data collection. SSRL is operated for the DOE and supported by OBER and NIH. We thank O. Lewinson and A. T. Lee for the cDNA of *Pa*ZntA, and Dr. Claudia Andreini (CERM, Magnetic Resonance Center, University of Florence, Italy) for support with MetalPDB analysis (http://metalweb.cerm.unifi.it/). We thank Prof. Douglas C. Rees (California Institute of Technology) and Prof. Poul Nissen (Aarhus University) for invaluable help in project development and discussions.

Supplementary Figure 1

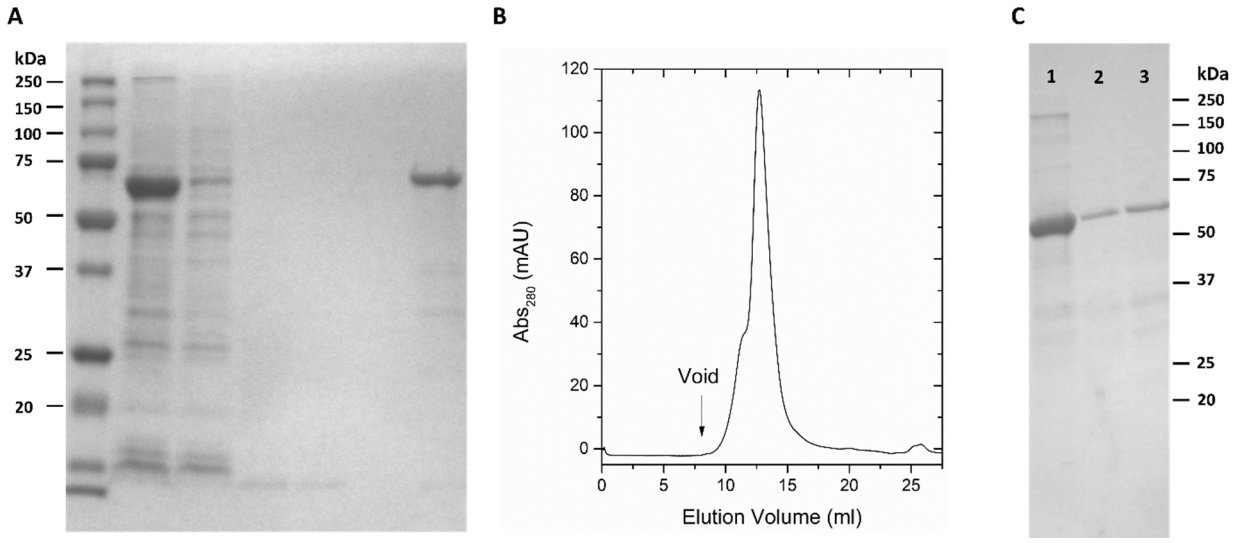

Figure S1: Purification of *P. aeuriginosa Pa*ΔZntA$_{121\text{-}740}$ and proteoliposome reconstitution of purified ΔZntA$_{121\text{-}740}$

(A) SDS-PAGE of the IMAC Ni-NTA affinity chromatography and desalting column runs. Lanes 1–7: Ladder, total membrane extract, flow-through, wash 1, wash 2, wash 3, eluted and rebuffered protein. The elution lane displays a prominent ~67kD band corresponding to *Pa*ΔZntA$_{121\text{-}740}$. (B) Size-exclusion profile of *Pa*ΔZntA$_{121\text{-}740}$ (0.5 mg/mL) on Superdex 200 10/30 column indicating monodispersity and absence of aggregated protein. (C) SDS-PAGE of *Pa*ΔZntA$_{121\text{-}740}$ in soluble detergent micelles (lane 1) and upon incorporation in proteoliposome lipid bilayers (lane 2, 0.5 µg; lane 3, 1 µg). For details on the proteoliposome reconstitution see *Materials and Methods.*

Supplementary Figure 2

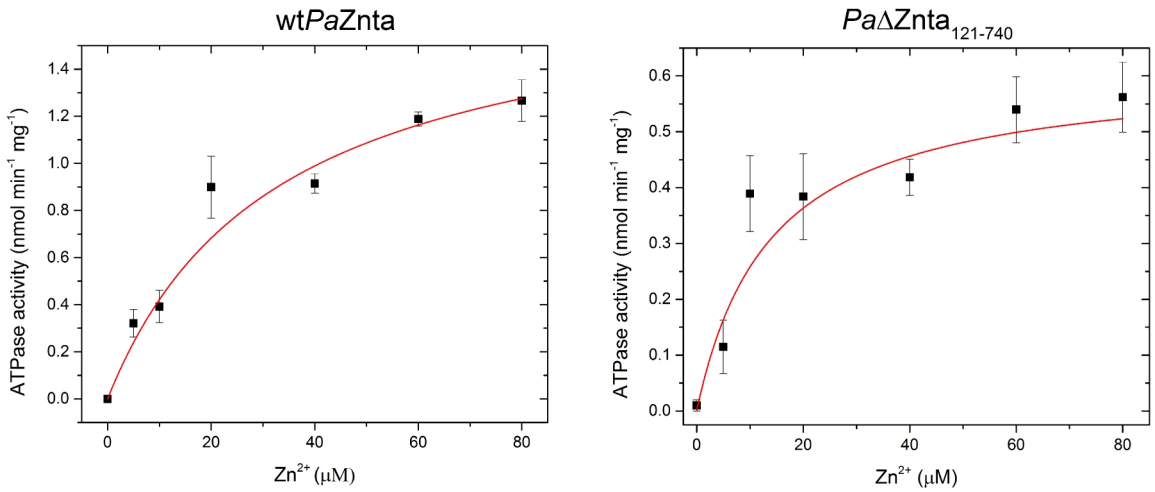

Figure S2: wt*Pa*ZntA and *Pa*ΔZntA$_{121-740}$ Zn(II)-dependent specific ATPase activity determined in Cymal-7 detergent micelles

The metal dependent ATPase activity was measured in the presence of increasing concentrations of Zn^{2+} ions, and data were fitted as described in *Materials and methods* using a Michaelis-Menten-type equation to derive V_{max} and $K_{M.}$

Supplementary Figure 3

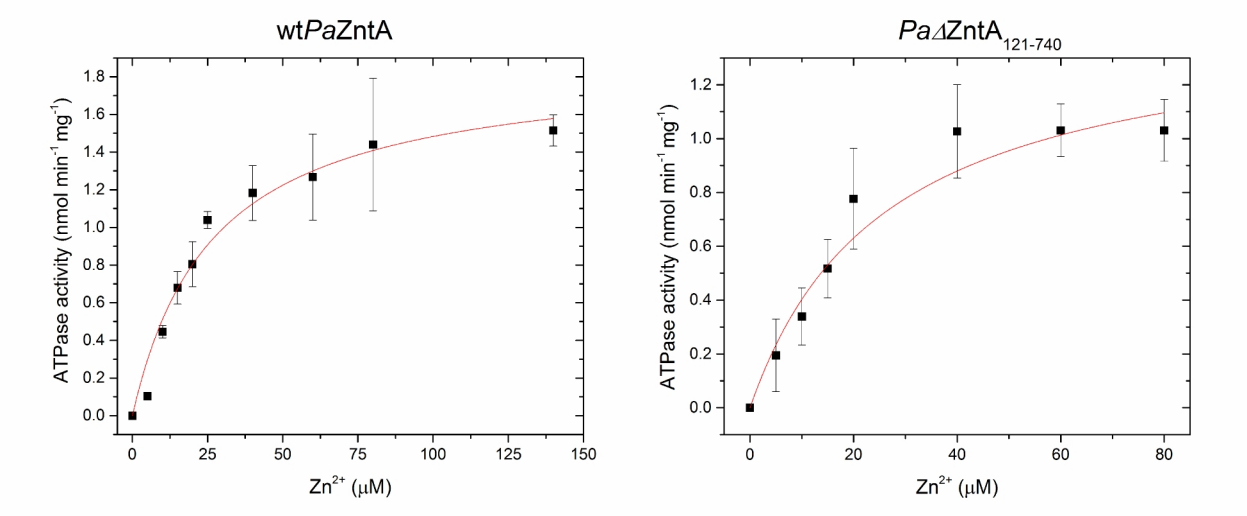

Figure S3: wt*Pa*ZntA and *Pa*ΔZntA$_{121-740}$ Zn(II)-dependent specific ATPase activity in artificial lipid bilayers (proteoliposomes)

The metal dependent ATPase activity was measured in the presence of increasing concentrations of Zn^{2+} ions, and data were fitted as described in *Materials and methods* using a Michaelis-Menten-type equation to derive V_{max} and $K_{M.}$

Supplementary Figure 4

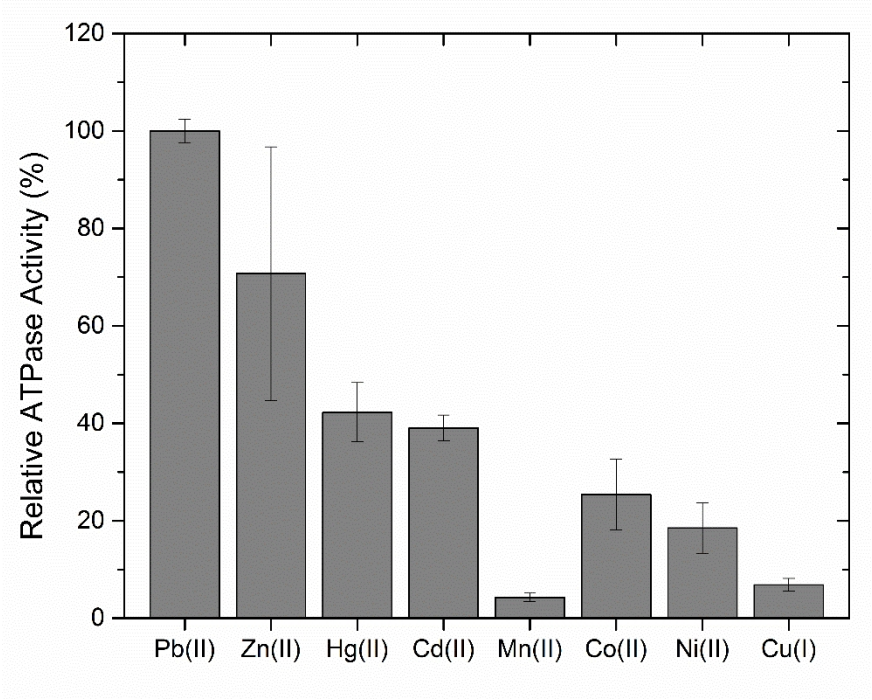

Figure S4: Metal selectivity of wt*Pa*ZntA as determined by metal-dependent stimulation of ATPase activity.

ATPase activity of detergent-solubilized wt*Pa*ZntA as a function of different metals ($Pb(CH_3COO)_2$, $ZnCl_2$, $HgCl_2$, $CdCl_2$, $MnCl_2$, $NiCl_2$, $CoCl_2$ or $CuCl_2$) determined using the Malachite Green assay as indicated in *Materials and Methods*.

Supplementary Figure 5

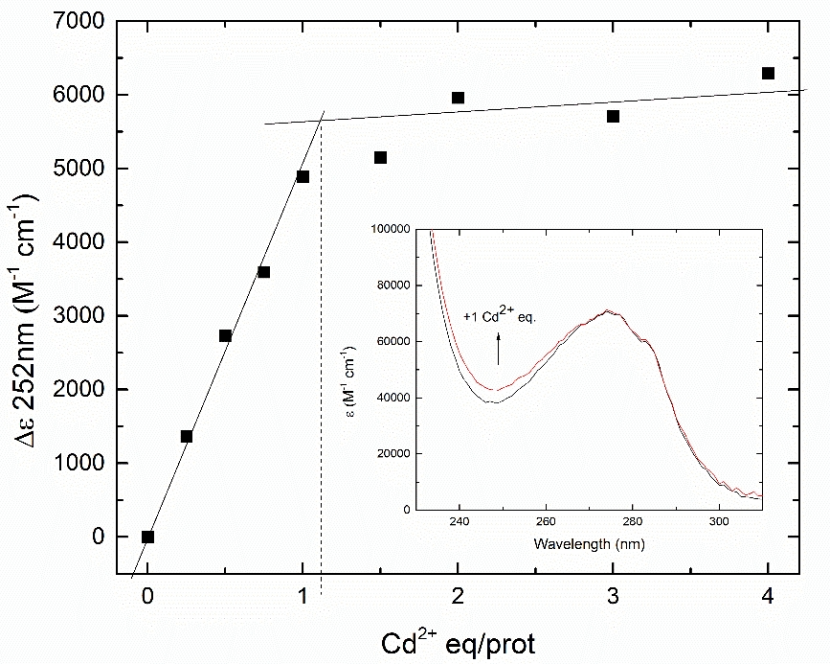

Figure S5: Cadmium binding to *Pa*ΔZntA$_{121-740}$ followed by electronic absorption spectroscopy.

The stepwise Cd^{2+} titration of *Pa*ΔZntA$_{121-740}$ was followed by UV-Vis absorption spectroscopy. Upon Cd^{2+} binding, the absorption spectra of ΔZntA$_{121-740}$-Cd^{2+} below 300 nm is characterized by a metal-induced charge-transfer envelope that overlays the backbone and aromatic residues transitions, indicative of ligand-to-metal charge transfer (LMCT) contributions from O/N and/or S ligands. The differential absorption between *Pa*ΔZntA$_{121-740}$-Cd^{2+} followed at 252 nm (CysS-Cd(II) LMCT) reveals a breakpoint at approx. 1 Cd(II) molar equivalent, indicating the presence of a single Cd^{2+} binding site. The insert shows the electronic absorption spectrum of apo*Pa*ΔZntA$_{121-740}$ and *Pa*ΔZntA$_{121-740}$-Cd^{2+} as a reference.

Supplementary Figure 6

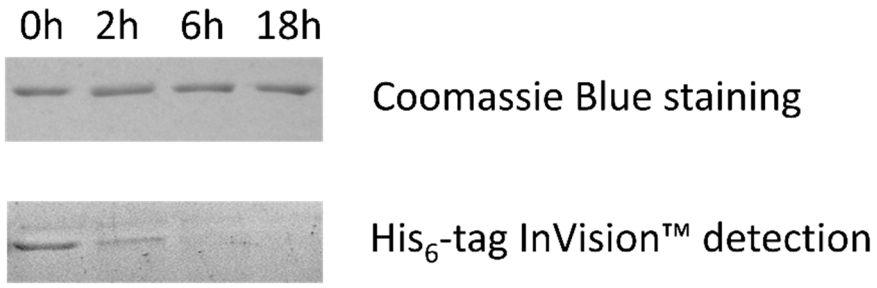

Figure S6: His_6-tag removal from *Pa*ΔZntA$_{121-740}$.

SDS-PAGE of purified His_6-ΔZntA$_{121-740}$ prior to thrombin cleavage (A) and optimization of the incubation time for efficient thrombin cleavage and tag removal by size exclusion chromatography (B) monitored by in-gel detection of the His_6-tag using In-Vision staining (Life Technologies) and subsequent Coomassie Blue staining.

Supplementary Figure 7

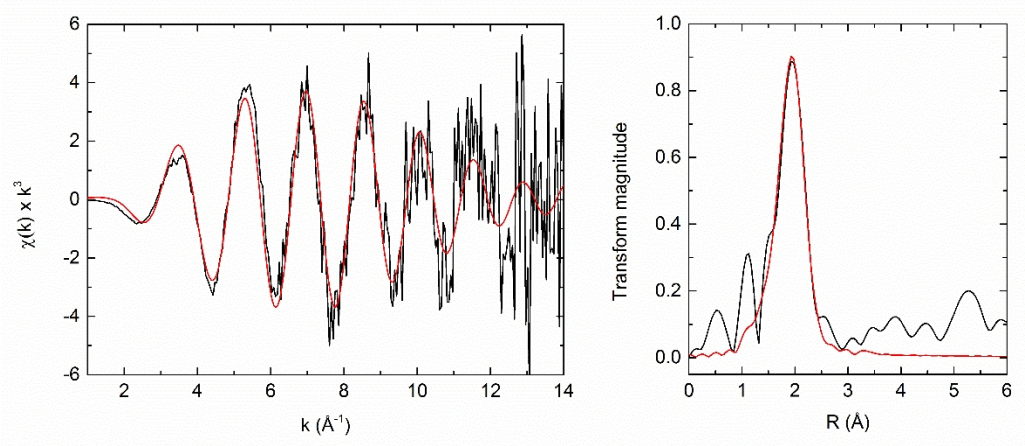

Figure S7: EXAFS and Fourier transforms of ΔZntA$_{121-740}$–Cd^{2+} in Cymal-7 micelles at extended k-range.

K-edge experimental EXAFS data (black line) and best fits (red line) with the corresponding Fourier transforms for ΔZntA$_{121-740}$–Cd^{2+} up to 14 Å^{-1} (low signal-to-noise). Extended X-ray absorption fine structure (EXAFS) best curve-fitting results are consistent with the model derived from fitting with a reduced k-range (reported in Figure 2 and Table 1)

Protein	M^{2+} eq. added	Scattering paths	N	R (Å)	σ^2 (Å^2)	F
ΔZnta-Cd^{2+}	1	Cd-S	2	2.531(9)	0.0026(5)	0.629
		Cd-N/O	2	2.29(1)	0.0018(9)	

Supplementary Figure 8

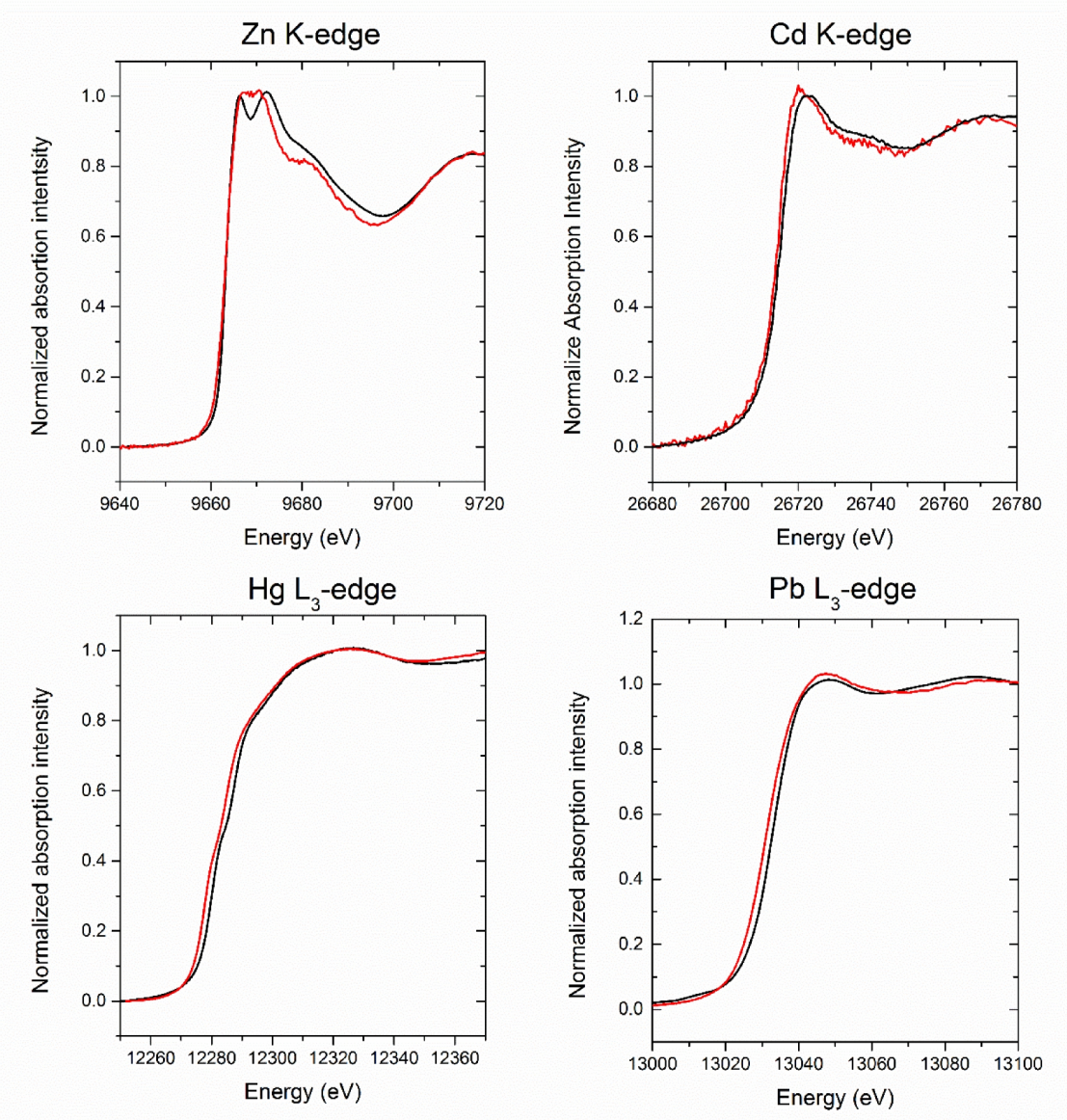

Figure S8: XANES spectra of ΔZntA$_{121\text{-}740}$–M^{2+}.

XANES spectra of ΔZntA$_{121\text{-}740}$–M^{2+} (M^{2+}= Zn^{2+}, Cd^{2+}, Hg^{2+} or Pb^{2+}) embedded in artificial lipid bilayers (proteoliposomes, red lines) compared to the spectra of ΔZntA$_{121\text{-}740}$–M^{2+} solubilized in Cymal-7 detergent micelles (black lines).

Supplementary Figure 9

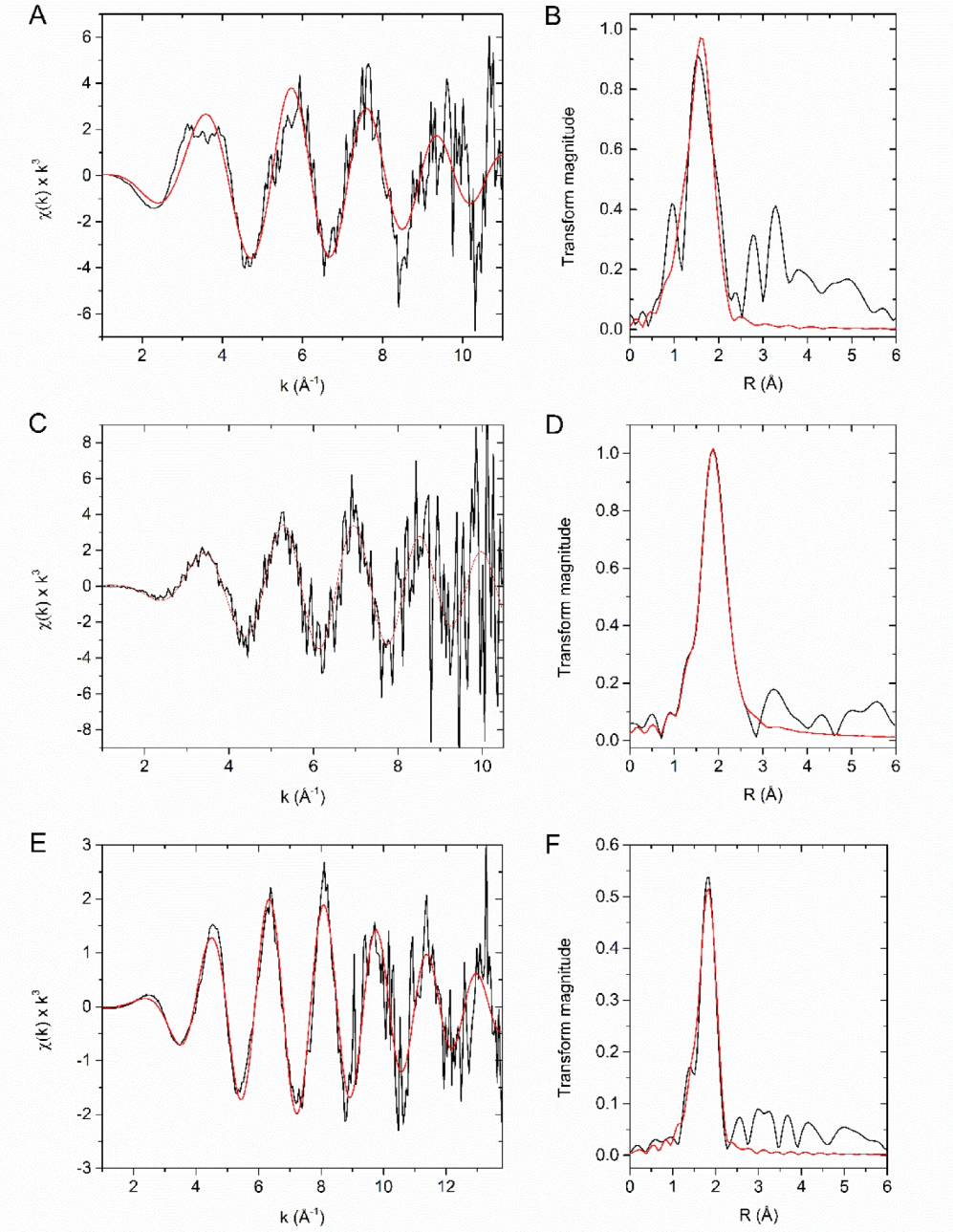

Figure S9: EXAFS and Fourier transforms of ΔZntA$_{121-740}$–Zn^{2+}, ΔZntA$_{121-740}$–Cd^{2+}, ΔZntA$_{121-740}$–Hg^{2+} embedded in lipid bilayers (proteoliposomes).

K-edge experimental EXAFS data (black line) and best fits (red line) with the corresponding Fourier transforms for ΔZntA$_{121-740}$–Zn^{2+} (A, B) and ΔZntA$_{121-740}$–Cd^{2+} (C, D). L_3-edge experimental EXAFS data (black line) and best fits (red line), with the corresponding Fourier transforms for

$\Delta ZntA_{121\text{-}740}$–$Hg^{2+}$ (E, F) embedded in proteoliposomes. The parameters for the best fits are listed in Table S1.

Supplementary Table 1

Table S1: Extended X-ray absorption fine structure (EXAFS) best curve-fitting results for the $\Delta ZntA_{121\text{-}740}$–$M^{2+}$ proteoliposomes

Protein	M^{2+} eq. added	Scattering paths	N	R (Å)	σ^2 (Å^2)	F
ΔZnta-Zn^{2+}	1	Zn-S	2	2.23(2)	0.007(1)	0.667
		Zn-N/O	2	1.99(3)	0.008(2)	
ΔZnta-Cd^{2+}	1	Cd-S	2	2.52(3)	0.001(1)	0.799
		Cd-N/O	2	2.26(4)	0.001(3)	
ΔZnta-Hg^{2+}	1	Hg-S	2	2.321(9)	0.0062(3)	0.495
		Hg-N/O	(2)	2.44(2)	0.02(2)	

Coordination numbers are indicated by N, interatomic distances R are given in Å, Debye-Waller factors σ^2 (the mean-square deviations in interatomic distance) in Å^2, and the fit-error function F is defined by $F = \sqrt{\Sigma\ k^6(\chi\ (k)_{calcd} - \chi\ (k)_{exp})^2 / \Sigma\ k^6(\chi\ (k)_{exp})^2}$ where $\chi(k)$ is the EXAFS oscillation and k is the photo-electron wave number. The values in parentheses are the standard deviations (± values on last digit) for best-fit parameters obtained by fitting the experimental data with the EXAFS equation utilizing the Marquardt algorithm.